Tuning the resonant frequencies of a drop by a magnetic field

Timothée Jamin, Yacine Djama, Jean-Claude Bacri, and Eric Falcon[*]

Université Paris Diderot, Sorbonne Paris Cité, MSC, CNRS (UMR 7057), 75013 Paris, France

We report an experimental study of a magnetic liquid drop deposited on a superhydrophobic substrate and subjected to vertical vibrations in the presence of a static magnetic field. It is well known that a flattened drop of usual liquid displays oscillating lobes at its periphery when vibrated. By adding ferromagnetic nanoparticles to a water drop and varying the strength of the magnetic field, we are experimentally able to efficiently tune the resonant frequencies of the drop. By using conservation energy arguments, we show that the magnetic field contribution is equivalent to adding an effective negative surface tension to the drop. Our model is found to be in good agreement with the experiments with no fitting parameter.

When a drop of liquid is dynamically driven by an external force, its free surface generally displays an oscillating pattern at the drop resonant frequency. At a fundamental level, the dynamical study of such an oscillating drop occurs in various domains at different scales. Indeed, liquid drop behavior is used to model stellar mass collisions or neutron-star oscillations in astrophysics [1] and nuclei in nuclear fission [2,3] or in cellular biology [4]. It is also involved in metrology for measuring viscosity of liquids [5] or surface tension of molten materials [6,7]. At a more practical level, it includes printing (ink drop generation), mixing of drop clouds, and droplet manipulations in microfluidic, optofluidic, and pharmaceutical industry [8]. Since the pioneer works of Rayleigh [9], the resonant frequencies of a drop have been studied experimentally by means of different forcing mechanisms: a water drop on a vibrating plate [10–13] or on a vibrating bath [14], in microgravity [15], by acoustic or air-flow levitation [16,17], by levitating it on its own vapor (Leidenfrost drops) [18–20], or by Lorentz force for a metal liquid drop [21,22]. A new challenge would be to accurately control and tune the free oscillations of a drop in a nonintrusive way. Notably, it would be of primary interest to be able to shift the resonant frequencies of the drop to avoid, for instance, some annoying frequency bands in practical situations.

In this Rapid Communication we study the dynamics of a flattened drop of magnetic fluid deposited on a superhydrophobic substrate vertically vibrated in the presence of a weak magnetic field of tunable amplitude. The fluid used is a ferrofluid consisting of a stable suspension of nanometric magnetic particles diluted in a carrier liquid (water). Above a critical acceleration of vibrations, the drop undergoes a parametric instability leading to an azimuthal pattern around the drop that oscillates at half the forcing frequency. A star-shaped drop is then observed made of several oscillating lobes. We observe that the resonant frequencies of the drop depend on the strength of the field. We show quantitatively and theoretically that we are able to shift these frequencies by tuning the effective surface tension of the drop through the field. Indeed, the contribution of the magnetic field is equivalent to the one of a negative surface tension. Including nanometric magnetic particles within a drop appears thus as a first step in being able to control and tune the free oscillations of a drop, such a magnetic fluid being known to shift the onsets of usual hydrodynamics instabilities (such as Kelvin-Helmholtz, Rayleigh-Taylor, or Rayleigh-Plateau ones) [23,24]. Finally, note that ferrofluid drop manipulation with a magnet is also an important task in microfluidics or laboratory on-chip technology [25–27] and in dynamic self-assembly phenomena [28].
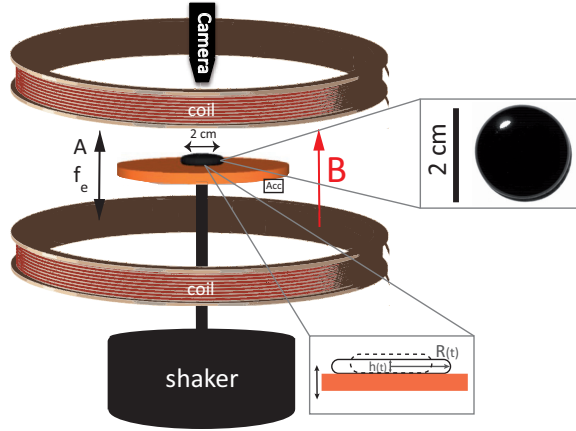
---

[*]eric.falcon@univ-paris-diderot.fr

FIG. 1. Experimental setup. The bottom inset shows a schematic of the puddle at two phases of the vibration. The top inset shows the top view of the ferrofluid puddle at rest.

The experimental setup is shown in Fig. 1. A volume of ferrofluid ($V = 1$ mL) is put on a plate. Due to gravity, the drop is flattened and looks like a puddle (radius $R = 9.7$ mm and thickness $h = 3.4$ mm; see the insets of Fig. 1). The plate was coated with a spray [29] to obtain a contact angle between the drop and the substrate measured of roughly $165°$. Such a superhydrophobic substrate is crucial to minimize the pinning force of the drop at the contact line and thus to obtain much better reproducible experiments [30,31]. The plate is then subjected to vertical sinusoidal vibrations by means of an electromagnetic shaker. The frequency and amplitude of vibrations are in the ranges $0 \leqslant f_e \leqslant 52$ Hz and $0 \leqslant A \leqslant 3$ mm, respectively. An accelerometer is fixed below the plate to measure the normalized acceleration of vibrations $\Gamma = A\omega_e^2/g$ with $\omega_e = 2\pi f_e$ and $g = 9.81$ m s^{-2} the acceleration of gravity. One has $0 \leqslant \Gamma \leqslant 4$. The ferrofluid puddle on the plate is placed between two horizontal coils (38 cm in mean diameter), generating a vertical static magnetic field B in the range $0 \leqslant B \leqslant 100$ G, 99% homogeneous in the horizontal plane [32]. The drop oscillations are recorded by means of a high-speed camera (PhantomV10) located above the drop, with a 1000 frames/s sampling and a 1600×1200 pixel resolution.

The ferrofluid used is an ionic aqueous suspension synthesized with 12.4% by volume of maghemite particles (Fe$_2$O$_3$, 7 ± 0.3 nm in diameter) [33]. The nanoparticle diameter and magnetic field values are small enough to avoid sedimentation or agglomeration due to vibrations, gravity, and magnetic fields [23]. The ferrofluid properties are density $\rho = 1550$ kg m^{-3}, surface tension $\gamma = 43 \pm 3$ mN m^{-1}, magnetic susceptibility $\chi(B) \approx \chi(B = 0) = 1.0$ [34], magnetic saturation, $M_{\text{sat}} = 36 \times 10^3$ A m^{-1}, and dynamic viscosity 1.4×10^{-3} N s m^{-2}. Its capillary length is then $l_c = \sqrt{\gamma/\rho g} = 1.7$ mm.

To accurately measure azimuthal drop oscillations, we use large flattened drops ($R \gg l_c$; see the bottom inset of Fig. 1). The Bond number, quantifying the ratio between gravity and capillary forces acting on the drop, is Bo $\equiv (R/l_c)^2 \simeq 33$. The ratio between magnetic and capillary forces is quantified by the magnetic Bond number Bo$_{\text{m}} \equiv B^2 R/\mu_0 \gamma$, with R the puddle radius and $\mu_0 = 4\pi \times 10^{-7}$ H m^{-1} the magnetic permeability of the vacuum. For our range of B, one has Bo$_{\text{m}} \leqslant 2$. Moreover, the magnetic effect is much smaller than that of gravity (Bo$_{\text{m}}/$Bo $\leqslant 0.06$), meaning that the strength of B is weak enough to not deform the flattened region of the puddle at rest.

We first carry out experiments with no magnetic field ($B = 0$). Figure 2 shows the parametric instability of a ferrofluid puddle subjected to vertical sinusoidal vibrations. Above a critical acceleration of vibration Γ_c, an azimuthal pattern is observed in the horizontal plane at the drop periphery: Lobes oscillate radially at half the forcing frequency $f_e/2$. When f_e is increased, the
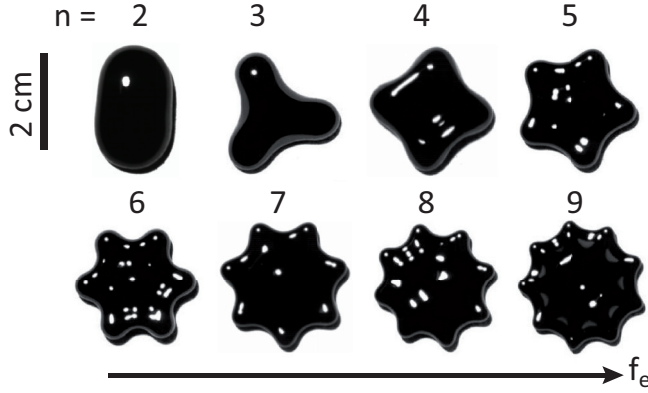
FIG. 2. Top view of the azimuthal pattern displayed around the drop as a function of f_e. Above a critical acceleration of vibration, an azimuthal pattern is observed normal to the vibration direction. When the forcing frequency f_e is increased ($0 \leqslant f_e \leqslant 52$ Hz), the number n of lobes, oscillating radially at $f_e/2$, increases from $n = 2$ to 9 (from left to right and top to bottom). See a movie in the Supplemental Material [35]. The magnetic field and the ferrofluid volume are $B = 0$ and $V \approx 1$ mL, respectively.

number n of oscillating lobes (mode number) increases from $n = 2$ to 9 as shown in Fig. 2 and the movie in the Supplemental Material [35].

The resonant frequencies f_n of such an inviscid drop are independent of the nature of the forcing and arise from an interplay between inertia and surface tension effects. In the limit $2R \gg h$, the flattened drop shape (see the inset of Fig. 1) is approximated by a cylindrical column of fluid. The radial amplitude of the lobes $a_n(t)$ is then governed by a harmonic oscillator equation of eigenfrequency f_n [9,36],

$$\frac{d^2 a_n(t)}{dt^2} + \omega_n^2 a_n(t) = 0, \quad \omega_n^2 = \frac{\gamma}{\rho R^3} n(n^2 - 1), \tag{1}$$

with $\omega_n = 2\pi f_n$.

A vertical sinusoidal vibration of the substrate is now applied to force the drop parametrically by modulating gravity $g \to g(t) = g[1 + \Gamma \cos(\omega_e t)]$ with $\Gamma = A\omega_e^2/g$. In addition, the thickness h of the puddle is usually given [10,13] by the quasistatic balance between gravity and capillary energies per unit volume ($2\gamma/h \simeq \rho g h/2$), i.e., $h \simeq 2l_c = 2\sqrt{\gamma/\rho g}$. The hypothesis of a constant volume of the puddle $V = \pi R^2 h$ then gives its radius $R = \sqrt{V/\pi h}$. Thus, a temporal modulation of gravity $g(t)$ induces those of the puddle thickness $h(t) \sim g(t)^{-1/2}$, radius $R(t) \sim h(t)^{-1/2} \sim g(t)^{1/4}$, and eigenfrequencies $\omega_n^2(t) \sim R(t)^{-3} \sim g(t)^{-3/4}$ using Eq. (1). For weak acceleration of vibrations $\Gamma \ll 1$, the parametric oscillator equation governing the amplitude of the lobes $a_n(t)$ then reads [10]

$$\frac{d^2 a_n(t)}{dt^2} + \omega_n^2 \left[1 - \frac{3}{4}\Gamma \cos(\omega_e t)\right] a_n(t) = 0. \tag{2}$$

Equation (2) is the Mathieu equation whose solutions are marginality curves (or instability tongues) separating stable zones (no deformation of the drop) and unstable zones where azimuthal standing waves at the drop periphery oscillate at half the forcing frequency $f_e/2$, near the resonant frequencies f_n [37]. This corresponds to the parametric instability shown in Fig. 2.

These tongues of instability are displayed in Fig. 3 in an acceleration-frequency phase space ($\Gamma_c/\Gamma_c^{\min}$ vs f_e) for $B = 0$ (open symbols). Data are obtained experimentally for various f_e by increasing Γ until we observe lobes at critical acceleration Γ_c; $\Gamma_c^{\min}$ is the minimum critical acceleration of each tongue. Equation (2) predicts that the minimum of each marginality curve
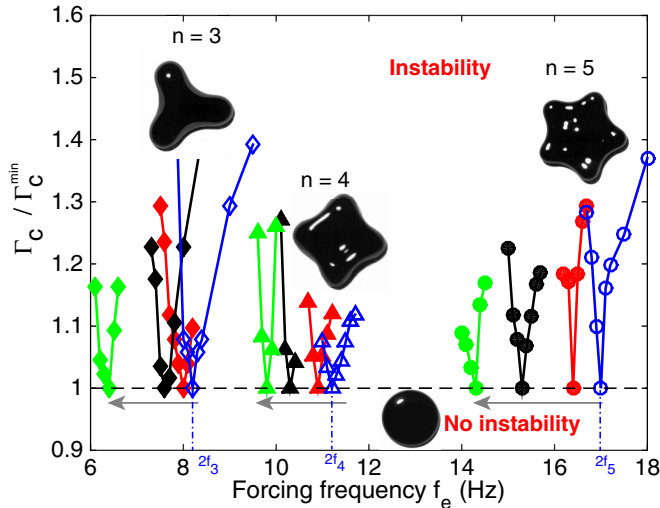
FIG. 3. Phase diagram of normalized rescaled critical acceleration $\Gamma_c/\Gamma_c^{\min}$ vs f_e. Curves are marginality curves separating stable and unstable zones for different mode numbers $n = 3$ ($\Diamond$), 4 ($\triangle$), and 5 ($\circ$). No instability occurs for $\Gamma \leqslant \Gamma_c$, whereas an azimuthal pattern around the puddle occurs within tongues. Open symbols corresponds to $B = 0$, closed symbols to $B \neq 0$: $B = 44$ [red (dark gray)], 77 (black), and 99 G [green (light gray)]. When B is increased (see arrows), the tongue are shifted towards a lower frequency, for each mode n.

occurs at twice the eigenmode $f_e = 2f_n$. Notice that experimental values for f_n are smaller than values given by Eq. (1). This difference ($<18\%$) may be explained by the fact that the quasistatic approximation yielding Eq. (2) is valid only for a low-frequency forcing. At higher frequency, the existence of axisymmetric modes shifts the minima of the marginality curves [38,39]. Indeed, we checked that this difference becomes negligible when we remove these axisymmetric modes by performing a control experiment with a superhydrophobic steady plate in contact with the drop top [40]. One can now wonder how an applied vertical magnetic field B affects the drop dynamics.

When B is increased for a fixed n, we observe that the instability tongue is shifted towards a lower frequency (see arrows in Fig. 3). The minimum of this curve and thus the eigenfrequency $f_n(B)$ are found to decrease with B. For $n = 5$, a relative shift of f_n of 16% is observed between extreme values of B used. One defines the absolute shift of the eigenfrequency as $\Delta\Omega_n(B) \equiv \omega_n^2(B = 0) - \omega_n^2(B)$, taking thus positive values. We plot in the inset of Fig. 4 the frequency shift $\Delta\Omega_n(B)$ as a function of B for different n. We find that $\Delta\Omega_n(B) \sim B^2$ for our range of B regardless of n. All data in the inset of Fig. 4 are found to collapse on a single curve when plotting $\Delta\Omega_n(B)$ as a function of $B^2 n^3$ (not shown). In order to compare with the model described below, $\Delta\Omega_n(B)$ is then displayed in Fig. 4 as a function of $B^2 n(n^2 - 1)$, noting that $n(n^2 - 1) \approx n^3$ for $n \geqslant 3$.

This frequency shift is not due to a geometrical effect mediated by B such as a drop lengthening along the field direction [24,41,42]. Indeed, using Eq. (1), a decrease of the puddle radius R with B (up to 6% here) would lead to an increase of the resonant frequency, a situation opposite to our observations (see Fig. 3). Moreover, the results of Fig. 4 are found again when adding a steady plate above the drop. Finally, note that no clear dependence of the critical acceleration $\Gamma_c^{\min}$ on B is observed.

An elegant way to understand the physical origin of the drop eigenfrequency shift with B is to balance energies involved in this system. In a first step, we assume $B = 0$ and follow Rayleigh model [9]. The flattened drop shape is approximated by a cylinder of fluid [see Fig. 5(a)]. We denote by $S_\perp$ its surface area normal to gravity and magnetic field (i.e., top plus bottom areas) and by $S_\parallel$ the peripheral surface area. At rest, they are denoted by $S_{\perp,0}$ and $S_{\parallel,0}$, respectively. We consider
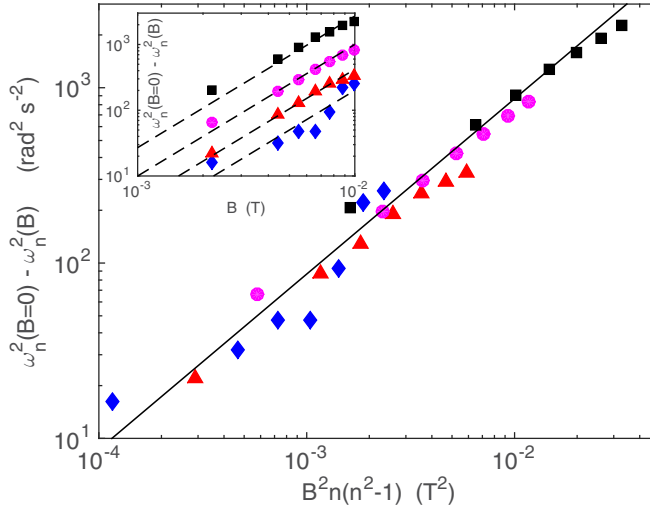
FIG. 4. Eigenfrequency shift $\omega_n^2(B=0) - \omega_n^2(B)$ as a function of $B^2 n(n^2 - 1)$ for different modes $n = 3$ (♦), 4 (▲), 5 (●), and 7 (■). The solid line is the prediction from the model of Eq. (10) with no fitting parameter. The inset shows an unrescaled frequency shift vs B. Dashed lines have a slope 2.

small radial deformations of the peripheral surface of amplitude $a_n(t) \ll R$ around an instantaneous radius $\bar{R}(t)$. In polar coordinates, this reads $r(\theta, t) = \bar{R}(t) + a_n(t) \cos(n\theta)$ [see Fig. 5(b)]. Here h is assumed constant with time and thus also $S_\perp$ due to volume conservation. It is known, since Rayleigh [9], that the radial deformation a_n induces an increase in $S_\parallel$ [see Figs. 5(a) and 5(b)] as

$$\Delta S_\parallel(t) \equiv S_\parallel(t) - S_{\parallel,0} = \frac{\pi h a_n^2(t)(n^2 - 1)}{2R}. \tag{3}$$

Thus, capillary energy increases by

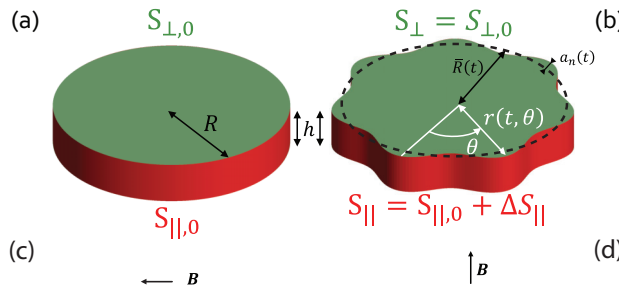$$\Delta E_c(t) = \gamma \Delta S_\parallel(t). \tag{4}$$

FIG. 5. Schematic view of the puddle. (a) At rest, the puddle is considered as a cylinder of liquid. (b) When lobes appear, the peripheral surface $S_\parallel$ increases as well as the capillary energy. Magnetization is illustrated within a ferrofluid film (c) parallel or (d) normal to $\mathbf{B}$.
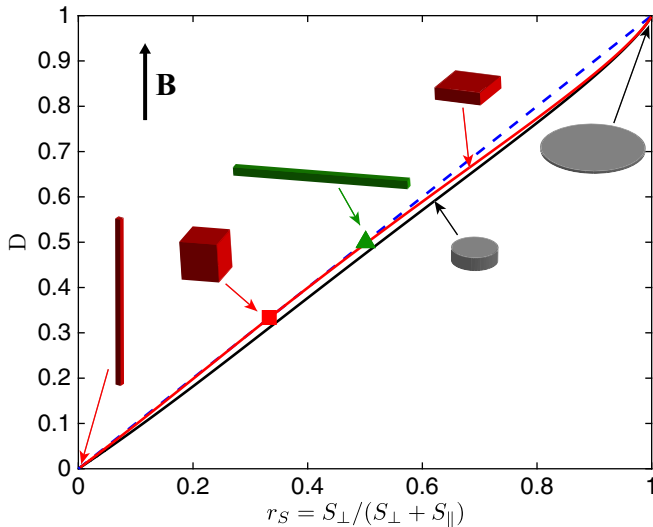
FIG. 6. Theoretical demagnetizing factors D vs surface ratio r_S. The black line is computed from the model in [43] for a cylinder of axis aligned with **B**; the red line (light gray) is computed from [44] for a square rod aligned with **B**; ■ is for a cube ($D = r_S = 1/3$ [44]); ▲ is for an infinitely elongated square rod normal to **B** ($D = r_S = 1/2$ [44]). The dashed line represents $D = r_S$ (slope 1).

In addition, the kinetic energy of the liquid reads

$$E_k(t) = \left(\frac{da_n}{dt}\right)^2 \frac{\pi \rho h R^2}{2n}. \tag{5}$$

The conservation of energy $d(E_k + E_c)/dt = 0$ then leads to Eq. (1) [9].

Let us now introduce the magnetic energy E_m in the Rayleigh model. For a linearly permeable ferrofluid of volume V [34], one has $E_m = -\mathbf{B} \cdot \int_V \mathbf{M} dV/2$, with **B** the external magnetic field and **M** the local ferrofluid magnetization [23]. The determination of **M** needs to take into account the ferrofluid boundary conditions. For instance, for a plane parallel to **B**, one has $E_m = -\chi V B^2/2\mu_0$ [see Fig. 5(c)] and for a plane normal to **B**, $E_m = -\chi V B^2/2\mu_0(1 + \chi)$ [see Fig. 5(d)]. Thus, the magnetic energy of a ferrofluid layer is smaller when **B** is parallel rather than normal to its surface.

For an arbitrary ferrofluid shape, **M** is nonuniform and an effective demagnetizing factor D is usually defined, with $0 \leqslant D \leqslant 1$ (depending on the shape), such that [23]

$$E_m = -\frac{\chi V B^2}{2\mu_0(1 + \chi D)}. \tag{6}$$

For volumes bounded by surfaces either parallel or normal to **B**, we can define the ratio between the surface area normal to **B** and the total surface area as $r_S \equiv S_\perp/(S_\perp + S_\parallel)$. Using known theoretical values of D for different geometries [43,44], we show in Fig. 6 that $D \approx r_S$ over the whole range of aspect ratios. This means that E_m decreases when the aspect ratio favors surfaces parallel to **B**, i.e., $D \to 0$ when $r_s \to 0$.

We can then replace the demagnetizing factor D by r_S in Eq. (6). The variation of $S_\parallel$ due to the presence of peripheral lobes induces a variation of E_m through r_S. Noticing that $S_{\perp,0} = 2\pi R^2$ and $S_{\parallel,0} = 2\pi Rh$ at rest, a first-order Taylor expansion in $\Delta S_\parallel$ for small deformations ($a_n \ll R$) leads to

$$\Delta E_m(t) = \gamma_m \Delta S_\parallel(t) \tag{7}$$

with

$$\gamma_m = -\frac{\chi^2 h B^2}{4\mu_0 (1 + \chi + h/R)^2}, \tag{8}$$

a quantity always negative. Then, using $\Delta S_{\parallel}$ from Eq. (3) and energies from Eqs (4), (5), and (7), the conservation of energy $d(E_k + E_c + E_m)/dt = 0$ finally leads to the resonant frequencies of the ferrofluid drop

$$\omega_n^2(B) = \frac{\gamma + \gamma_m(B^2)}{\rho R^3} n(n^2 - 1). \tag{9}$$

Using Eq. (1) then leads to

$$\omega_n^2(B = 0) - \omega_n^2(B) = -\frac{\gamma_m(B^2)}{\rho R^3} n(n^2 - 1). \tag{10}$$

The $B^2 n(n^2 - 1)$ scaling is in good agreement with the one found experimentally (see Fig. 4) as well as for the theoretical prefactor with no fitting parameter.

Notice that Eq. (9) includes the usual capillary contribution γ and a magnetic one γ_m that depends on B. The magnetic term thus plays the role of a negative surface tension ($\gamma_m < 0$) that thus reduces the drop resonant frequencies. The magnetic field can be then used to tune the effective surface tension $\gamma_{\text{eff}} \equiv \gamma + \gamma_m$ and thus ω_n. For our ranges of B, using ferrofluid properties and geometry, one has $\gamma_m \in [-8.5, 0]$ mN m^{-1}, which is up to 20% of γ. The analogy with surface tension arises from $\Delta E_m = \gamma_m(B^2)\Delta S_{\parallel}$. This means that an increase of the drop surface area parallel to **B** favors its magnetization and thus decreases E_m since $\gamma_m < 0$. Consequently, B has a stabilizing effect on the lobes. Finally, note that a model of the dynamics of a ferrofluid drop confined between two plates [45,46] mentioned such a possible negative surface tension effect, but requires $\chi \ll 1$ and thus cannot apply here where $\chi = 1$.

To conclude, we have studied the dynamics of parametric oscillations of a centimetric ferrofluid drop on a superhydrophobic plate subjected to vertical sinusoidal vibrations and a constant magnetic field. By adding ferromagnetic nanoparticles to a water drop, we are able to shift significantly its eigenfrequencies by tuning the magnetic field strength. Using energy conservation, we extend the Rayleigh model and show that the resonant frequency shift is well captured by our model with no fitting parameter. We also show that the magnetic field acts as a negative surface tension and is a way to tune the effective surface tension of the drop. Finally, the weakness of the field strength and the small size of ferromagnetic particles are favorable to miniaturization to plan to control the oscillations of centimeter-to-microscale drop in a new nonintrusive way for potential applications.

[1] R. H. Durisen, R. A. Gingold, J. E. Tohline, and A. P. Boss, Dynamic fission instabilities in rapidly rotating $n = 3/2$ polytropes—A comparison of results from finite-difference and smoothed particle hydrodynamics codes, Astrophys. J. **305**, 281 (1986).

[2] A. A. Amsden, G. F. Bertsch, F. H. Harlow, and J. R. Nix, Relativistic Hydrodynamic Theory of Heavy-Ion Collisions, Phys. Rev. Lett. **35**, 905 (1975).

[3] J. A. Zingman, T. L. McAbee, J. R. Wilson, and C. T. Alonso, Collective sow and pion production in a hydrodynamic model, Phys. Rev. C **38**, 760 (1988).

[4] C. P. Brangwynne, T. J. Mitchison, and A. A. Hyman, Active liquid-like behavior of nucleoli determines their size and shape in Xenopus laevis oocytes, Proc. Natl. Acad. Sci. USA **108**, 4334 (2011).

[5] M. Papoular and C. Parayre, Gas-Film Levitated Liquids: Shape Fluctuations of Viscous Drops, Phys. Rev. Lett. **78**, 2120 (1997).

[6] M. E. Fraser, W.-K. Lu, A. E. Hamielec, and R. Murarka, Surface tension measurements on pure liquid iron and nickel by an oscillating drop technique, Metall. Trans. **2**, 817 (1971).

[7] M. Przyborowski, T. Hibiya, M. Eguchi, and I. Egry, Surface tension measurement of molten silicon by the oscillating drop method using electromagnetic levitation, J. Cryst. Growth **151**, 60 (1995).

[8] J. M. Oh, D. Legendre, and F. Mugele, Shaken not stirred—On internal flow patterns in oscillating sessile drops, Europhys. Lett. **98**, 34003 (2012).

[9] Lord Rayleigh, On the capillary phenomena of jets, Proc. R. Soc. London **29**, 71 (1879).

[10] N. Yoshiyasu, K. Matsuda, and R. Takaki, Self-induced vibration of a water drop placed on an oscillating plate, J. Phys. Soc. Jpn. **65**, 2068 (1996).

[11] M. Okada and M. Okada, Observation of the shape of a water drop on an oscillating Teflon plate, Exp. Fluids **41**, 789 (2006).

[12] X. Noblin, A. Buguin, and F. Brochard-Wyart, Vibrations of sessile drops, Eur. Phys. J. Spec. Top. **166**, 7 (2009).

[13] P. Brunet and J. H. Snoeijer, Star-drops formed by periodic excitation and on an air cushion—A short review, Eur. Phys. J. Spec. Top. **192**, 207 (2011).

[14] S. Dorbolo, D. Terwagne, N. Vandewalle, and T. Gilet, Resonant and rolling droplet, New J. Phys. **10**, 113021 (2008).

[15] R. E. Apfel, Y. Tian, J. Jankovsky, T. Shi, X. Chen, R. G. Holt, E. Trinh, A. Croonquist, K. C. Thornton, A. Sacco, C. Coleman, F. W. Leslie, and D. H. Matthiesen, Free Oscillations and Surfactant Studies of Superdeformed Drops in Microgravity, Phys. Rev. Lett. **78**, 1912 (1997).

[16] C. L. Shen, W. J. Xie, and B. Wei, Parametrically excited sectorial oscillation of liquid drops floating in ultrasound, Phys. Rev. E **81**, 046305 (2010).

[17] W. Bouwhuis, K. G. Winkels, I. R. Peters, P. Brunet, D. van der Meer, and J. H. Snoeijer, Oscillating and star-shaped drops levitated by an airflow, Phys. Rev. E **88**, 023017 (2013).

[18] N. J. Holter and W. R. Glasscock, Vibrations of evaporating liquid drops, J. Acoust. Soc. Am. **24**, 682 (1952).

[19] A. Snezhko, E. Ben Jacob, and I. S. Aranson, Pulsating gliding transition in the dynamics of levitating liquid nitrogen droplets, New J. Phys. **10**, 043034 (2008).

[20] K. Piroird, B. D. Texier, C. Clanet, and D. Quéré, Reshaping and capturing Leidenfrost drops with a magnet, Phys. Fluids **25**, 032108 (2013).

[21] Y. Fautrelle, J. Etay, and S. Daugan, Free-surface horizontal waves generated by low-frequency alternating magnetic fields, J. Fluid Mech. **527**, 285 (2005).

[22] V. Kocourek, C. Karcher, M. Conrath, and D. Schulze, Stability of liquid metal drops affected by a high-frequency magnetic field, Phys. Rev. E **74**, 026303 (2006).

[23] R. E. Rosensweig, *Ferrohydrodynamics* (Dover, New York, 1997).

[24] E. Blums, A. Cebers, and M. M. Maiorov, *Magnetic Fluids* (de Gruyter, Berlin, 1997).

[25] E. Bormashenko, R. Pogreb, Y. Bormashenko, A. Musin, and T. Stein, New investigations on ferrofluidics: Ferrofluidic marbles and magnetic-field-driven drops on superhydrophobic surfaces, Langmuir **24**, 12119 (2008).

[26] V. Sterr, R. Krau, K. I. Morozov, I. Rehberg, A. Engel, and R. Richter, Rolling ferrofluid drop on the surface of a liquid, New J. Phys. **10**, 063029 (2008).

[27] N.-T. Nguyen, G. Zhu, Y.-C. Chua, V.-N. Phan, and S.-H. Tan, Magnetowetting and sliding motion of a sessile ferrofluid droplet in the presence of a permanent magnet, Langmuir **26**, 12553 (2010).

[28] J. V. I. Timonen, M. Latikka, L. Leibler, R. H. A. Ras, and O. Ikkala, Switchable static and dynamic self-assembly of magnetic droplets on superhyrophobic surfaces, Science **341**, 253 (2013).

[29] Ultra Ever Dry© spray; see http://ultraeverdry-tap.com/index.html

[30] F. Celestini and R. Kofman, Vibration of submillimeter-size supported droplets, Phys. Rev. E **73**, 041602 (2006).

[31] C.-T. Chang, J. B. Bostwick, P. H. Steen, and S. Daniel, Substrate constraint modifies the Rayleigh spectrum of vibrating sessile drops, Phys. Rev. E **88**, 023015 (2013).

[32] The coils are in quasi-Helmholtz configuration and cooled with water circulation; see J. Browaeys, J.-C. Bacri, C. Flament, S. Neveu, and R. Perzynski, Surface waves in ferrofluids under vertical magnetic field, Eur. Phys. J. B **9**, 335 (1999).

[33] The ferrofluid synthesis has been performed by the Laboratory LI2C, University Pierre et Marie Curie—Paris 6 according to Massart's method: R. Massart, Preparation of aqueous magnetic liquids in alkaline and acidic media, IEEE Trans. Magn. **17**, 1247 (1981).

[34] For our range of values of B, the magnetic susceptibility of the ferrofluid $\chi(B)$ varies less than 3%, thus one fixes $\chi(B) = \chi(B = 0)$.

[35] See Supplemental Material at http://link.aps.org/supplemental/10.1103/PhysRevFluids.1.021901 for an illustrative movie of oscillations of a ferrofluid puddle ($R \simeq 1$ cm in radius) on a superhydrophobic plate (top view). When the vibrating plate frequency increases, the eigenmode number n increases, showing azimuthal waves constituting of n lobes oscillating radially. The vibration acceleration $0 \leqslant \Gamma \leqslant 4$ and magnetic field $B = 0$.

[36] H. Lamb, *Hydrodynamics*, 6th ed. (Dover, New York, 1932).

[37] J. Mathews and R. L. Walker, *Mathematical Methods of Physics*, 2nd ed. (Addison-Wesley, New York, 1969), pp. 198–204.

[38] X. Noblin, A. Buguin, and F. Brochard-Wyart, Triplon Modes of Puddles, Phys. Rev. Lett. **94**, 166102 (2005).

[39] X. Noblin, A. Buguin, and F. Brochard-Wyart, Vibrated sessile drops: Transition between pinned and mobile contact line oscillations, Eur. Phys. J. E **14**, 395 (2004).

[40] T. Jamin, Ph.D. thesis, Université Paris–Diderot, 2016.

[41] V. I. Arkhipenko, Yu. D. Barkov, and V. G. Bashtovoi, Shape of a drop of magnetized fluid in a homogeneous magnetic field, Magnetohydrodynamics **14**, 373 (1978).

[42] J.-C. Bacri and D. Salin, Instability of ferrofluid magnetic drops under magnetic field, J. Phys. Lett. (France) **43**, L649 (1982).

[43] A. S. Arrott, B. Heinrich, T. L. Templeton, and A. Aharoni, Micromagnetics of curling configurations in magnetically soft cylinders, J. Appl. Phys. **50**, 2387 (1979).

[44] A. Aharoni, Demagnetizing factors for rectangular ferromagnetic prisms, J. Appl. Phys. **83**, 3432 (1998).

[45] S. A. Langer, R. E. Goldstein, and D. P. Jackson, Dynamics of labyrinthine pattern formation in magnetic fluids, Phys. Rev. A **46**, 4894 (1992).

[46] D. P. Jackson, R. E. Goldstein, and A. O. Cebers, Hydrodynamics of fingering instabilities in dipolar fluids, Phys. Rev. E **50**, 298 (1994).